Eur. Phys. J. D (2017) 71: 172
DOI: 10.1140/epjd/e2017-80072-3

THE EUROPEAN PHYSICAL JOURNAL D

Regular Article

# Localized structures and spatiotemporal chaos: comparison between the driven damped sine-Gordon and the Lugiato-Lefever model*

Michel A. Ferré[1], Marcel G. Clerc[1,a], Saliya Coulibally[2], René G. Rojas[3], and Mustapha Tlidi[4]

[1] Departamento de Física, FCFM, Universidad de Chile, Casilla 487-3 Santiago, Chile
[2] Université de Lille, CNRS, UMR 8523 - PhLAM - Physique des Lasers Atomes et Molécules, 59000 Lille, France
[3] Intituto de Física, Pontificia Universidad Católica de Valparaíso, Casilla 4059, Valparaíso, Chile
[4] Faculté des Sciences, Université Libre de Bruxelles (U.L.B.), CP 231, Campus Plaine, 1050 Bruxelles, Belgium

Received 31 January 2017 / Received in final form 11 April 2017
Published online 22 June 2017 – 

**Abstract.** Driven damped coupled oscillators exhibit complex spatiotemporal dynamics. An archetype model is the driven damped sine-Gordon equation, which can describe several physical systems such as coupled pendula, extended Josephson junction, optical systems and driven magnetic wires. Close to resonance an enveloped model in the form Lugiato-Lefever equation can be derived from the driven damped sine-Gordon equation. We compare the dynamics obtained from both models. Unexpectedly, qualitatively similar dynamical behaviors are obtained for both models including homogeneous steady states, localized structures, and pattern waves. For large forcing, both systems share similar spatiotemporal chaos.

## 1 Introduction

In their seminal paper, Lugiato and Lefever introduce for the first time the mean field approach to derive a simple model to describe the spatiotemporal evolution of the intracavity field envelope [1]. An early report on transverse patterns, which describes numerical simulations of self-focusing and filamentation of light beams in bistable nonlinear media [2,3]. Later on Lugiato and Lefever, have shown that the existence of transverse patterns does not require a bistable homogeneous steady state [1]. They show that the symmetry breaking instability leading to the spontaneous formation of stationary spatial patterns can occur in the monostable regime far from any second-order critical point. More importantly, they have established the link between the well known symmetry-breaking instability in chemical reaction diffusion systems [4–6] and the transverse pattern in nonlinear optics [1]. This instability is often called Turing-Prigogine instability [4,5] that causes a spontaneous transition from a spatially uniform state to stationary spatially periodic patterns with an intrinsic wavelength. This quantity is determined by dynamical parameters such as kinetic parameters and diffusion coefficients and not by the system physical dimensions or geometrical constraints.

The Lugiato-Lefever equation (LLE) have broad applicability than passive optical cavities and it is a well-known paradigm in the study of spatial periodic or localized patterns. It has been considered for that purpose in diffractive systems such as liquid crystals, left-handed materials [7], and photonics coupled waveguides [8]. It has been also derived for dispersive systems such as nonlinear fiber resonator [9] and whispering-gallery-mode microresonators leading to optical frequency comb generation [10–12]. Diffractive and dispersive cavity leading to three dimensional LLE have been analyzed in [13–15]. The LLE is a cubic nonlinear Schrödinger equation, including damping, detuning and driving effect. This amplitude equation has been derived in early reports to describe the plasma driven by an external radio frequency field [16,17] and the condensate in the presence of an applied ac field [18]. An analytical study of stability and bifurcation of the spatially dependent time solution of the LLE has been performed at the conservative limit [19].

The aim of this paper is to show that the dynamics predicted by the Lugiato-Lefever equation could also be applied to two non-optical systems, namely a forced dissipative chain of pendula and a driven extended Josephson junction. Both systems are schematically depicted in Figure 1. It is well known that the spatiotemporal evolution of these systems is ruled by the driven dissipative sine-Gordon model. We perform qualitative a comparison between the Lugiato-Lefever and the driven dissipative sine-Gordon models. Far from the conservative limit, a single envelope approximation is no longer

* Contribution to the Topical Issue: "Theory and Applications of the Lugiato-Lefever Equation", edited by Yanne K. Chembo, Damia Gomila, Mustapha Tlidi, Curtis R. Menyuk.

[a] e-mail: marcel@dfi.uchile.cl

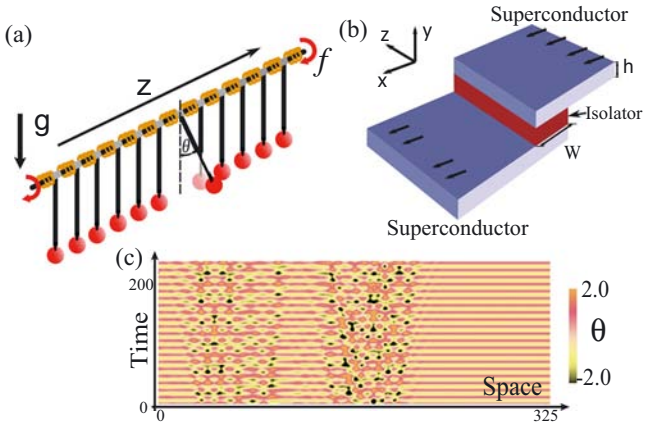


**Fig. 1.** Driven damped nonlinear oscillators. (a) Schematic representation of a driven dissipative chain of pendula. $\theta$ is the angle formed by a pendulum and the vertical axis; $f = \gamma \sin(\omega t)$ accounts for an temporal modulating torque with an amplitude and frequency $\gamma$ and $\omega$, respectively. (b) Schematic representation of an extended Josephson junction, which is composed of two superconductors separated by an insulating strip. (c) Spatiotemporal evolution of a driven damped sine-Gordon equation (1), by $\omega_0 = 1$, $\mu = 0.05$, $\kappa = 1$, $\gamma = 5.9$, $\omega = 2.7$, $dt = 0.05$ and $dx = 0.65$.

governed by the Lugiato-Lefever equation. Unexpectedly, one observes a qualitatively similar bifurcation diagram for homogeneous, localized and pattern states, even spatiotemporal chaotic dynamical behaviors. The Lyapunov spectrum is used to characterize the complex spatiotemporal dynamics presented by a driven dissipative sine-Gordon model.

The paper is organized as follows. After a historical perspective, we present in Section 2, the derivation of LLE equation from a forced dissipative sine-Gordon model. Then in Section 3, we discuss the dynamics of the LLE versus a forced dissipative chain of pendula including localized structures, pattern waves and spatiotemporal chaos. Finally, in Section 4, we conclude and we provide some comments.

## 2 The driven dissipative chain of pendula

### 2.1 Historical perspective

The main characteristic of an oscillator is to possess an intrinsic natural frequency. The forcing at this particular frequency is the natural way to excite an oscillator in an efficient way. When forcing an oscillator close to its natural frequency, the oscillator exhibits a large oscillation amplitude, which can be understood from a balance between the injection (forcing) and the dissipation of energy (dissipation). This is a *resonance* phenomenon [20]. The resonance phenomenon has been known since the dawn of modern science by Galileo [21], who was interested in the understanding of the pendulum dynamics. Depending on the intensity and the frequency of the forcing this oscillator begins to manifest its nonlinear nature, with an asymmetric amplitude response with respect to the forcing frequency [20]. Likewise, by sufficiently large forcing intensity the oscillator can exhibit bistability between two equilibrium oscillations [20]. When increasing the forcing amplitude, the system may exhibit complex chaotic type behaviors (see the textbook [22] and reference therein). The previous scenario changes drastically when one considers a spatial extension of the nonlinear oscillator. In the latter case one expects the emergence of patterns, localized solutions, fronts, nonlinear waves, chaos, chimera states, phase turbulence, spatiotemporal chaos, weak turbulence, among others. Due to the complexity of the nonlinear partial differential equations, only particular models close to conservative limits have been studied analytically in detail (cf. Ref. [23] and references therein). A systematic study a chain of forced oscillators through *amplitude equations* [24]. This type of approach is valid for small amplitude that has allowed a unified understanding of several phenomena such as pattern formation, localized structures, phase turbulence, defect turbulence, spatiotemporal chaos, weak turbulence, among others.

In optics a natural nonlinear extended oscillators are cavities [1]. Therefore, by means of external electromagnetic waves with a frequency near to the cavity frequency, one expects to be able to resonate this optical cavity with the injection. A simplified amplitude equation that describes the dynamics of a forced Kerr optical cavities close to resonance is the Lugiato-Lefever equation [1].

### 2.2 From driven damped sine-Gordon model to Lugiato-Lefever equation

Let us consider a driven damped chain of pendula (cf. Fig. 1a), which is described, in the continuum limit, by a following forced dissipative sine-Gordon equation

$$\ddot{\theta}(z,t) = -\omega_o^2 \sin\theta - \mu\dot{\theta} + k\partial_{zz}\theta + \gamma \sin(\omega t), \qquad (1)$$

where $\theta(z,t)$ is the angle formed by a pendulum and the vertical axis in the $z$-position at time $t$; $\omega_o$ is the natural frequency of the pendulum; $\mu$, $k$, $\gamma$, and $\omega$ are the damping, elastic coupling, amplitude and frequency of the forcing, respectively. For the sake of simplicity, we have chosen a harmonic external forcing. The model equation (1) takes into account of the dynamics of a chain of coupled pendula to first neighbors by restitution springs [25], which are mounted on the horizontal bar that oscillates in a harmonic way with respect to its azimuthal axis (cf. Fig. 1a). Hence, the bar induces an oscillatory torque on each pendulum.

The model equation (1) can be applied to another physical system, namely an extended Josephson [25,26]. The schematic of this system is depicted in Figure 1b. In the following we provide the meaning of the variable and the parameters of the extended Josephson. The variable $\theta(z,t)$ in equation (1) accounts for the phase difference between the wave function of each superconductor. The parameter $\omega_o^2$ stands for the superconductor current in the junction and its value is determined by the particular characteristics of the junction. The parameter $\mu$

accounts for the normal current, and the parameter $k$ is proportional to the square of light speed. The term proportional to $\gamma$ in equation (1) takes into account of the alternating current across the junction. Indeed, modifications of the sine-Gordon equation allows to describe different physical systems such as charge density waves [27], dislocations in crystal [28], magnetization of driven ferromagnetic wires [29], gravity and high-energy [25].

For zero forcing and damping, $\gamma = \mu = 0$, the above model describes a Hamiltonian system, that present time reversal invariance, which is well-known as the sine-Gordon model. Figure 1 illustrates a schematic representation of a driven dissipative chain of pendula. When the dissipation is included, the vertical state $\theta(z,t) = 0$ becomes the only stable equilibrium. The forcing induces oscillations of the vertical state with the forcing frequency. The amplitude of this oscillation strongly depends on the detuning between the forcing and natural frequency, $\nu \equiv \omega - \omega_0$. Figure 1c shows a complex spatiotemporal evolution of the driven damped sine-Gordon equation. All numerical simulations were conducted using finite differences code to first neighbors with the fourth-order Runge-Kutta algorithm and Neumann boundary conditions. The spatial and temporal discretization are considered in the continuous limit.

### 2.3 Envelop approximation

To figure out the dynamics observed in the driven damped sine-Gordon equation, we consider the quasi-reversal limit, that is, the time reversal limit perturbed with small injections and small dissipations of energy [30–32]. In this limit, model (1) corresponds to a perturbed sine-Gordon equation with $\nu \sim \mu \sim \varepsilon$, $\gamma \sim \varepsilon^{3/2}$, and $\varepsilon$ is an arbitrary small scaling parameter, $\varepsilon \ll 1$. Considering the following ansatz

$$\theta = \sqrt{\frac{2\varepsilon}{3\omega_o}} A(x,\tau) e^{i\omega t} + \left(\frac{\varepsilon}{6\omega_0}\right)^{3/2} A^3 e^{i3\omega t} + c.c. + h.o.t, \tag{2}$$

where $A(x,\tau)$ is the slowly varying envelope of the vertical state, $\tau \equiv \varepsilon t$ and $x \equiv \sqrt{2\varepsilon\omega_0/k}z$ are slow variables, $c.c.$ and $h.o.t.$ denote the complex conjugate and the high order terms in amplitude $A$, respectively. Introducing the above ansatz in equation (1), and matching different orders in $\varepsilon$. After straightforward calculations, at the dominant order in $\varepsilon$, the envelope $A$ obeys the Lugiato-Lefever equation

$$\partial_\tau A = -(\tilde{\mu} + i\nu)A - i\,|A|^2 A - i\partial_x^2 A - \tilde{\gamma}, \tag{3}$$

where $\tilde{\mu} \equiv \mu/2$, and $\tilde{\gamma} \equiv \gamma/4\sqrt{2\omega/3}$. Notice that the terms of above equation are of order $\varepsilon^{3/2}$ and the higher order terms are at least of order $\varepsilon^{5/2}$. The above amplitude equation is the paradigmatic one-dimensional Lugiato-Lefever equation [1] or the driven damped nonlinear Schrödinger equation [16–18]. The correspondence between the sine-Gordon model and the Lugiato-Lefever equation was established in reference [33]. The sign of the second derivative with respect the $x$ coordinate is negative and the nonlinearity is of the focusing type. Depending on the context in which the Lugiato-Lefever equation is derived, the sign of nonlinearity and dispersion or diffraction can be positive or negative see classification in Table 1. In optics the LLE model was derived considering the mean field limit of driven Kerr cavities with a high Fresnel number-assuming that the cavity is much shorter than the diffraction and the nonlinearity spatial scales.

**Table 1.** Sign of diffraction, dispersion and nonlinearity. Passive cavity [1], diffraction is always positive while nonlinearity can be either positive or negative. Cavity filled with left-handed materials (LHM), diffraction and nonlinearity can be either positive or negative [7]. Whispering-gallery-mode microresonators (WGM) leading to optical frequency comb generation [10–12]. In the case of the chain of pendula both nonlinearity and dispersion are negative.

| | Diffraction | Dispersion | Nonlinearity |
|---|---|---|---|
| Passive cavity | + | | ± |
| LHM | ± | | ± |
| Nonlinear Fiber | | ± | + |
| WGM | | + | ± |
| Chain of pendula | | − | − |
| Josephson Junctions | | − | − |

The Lugiato-Lefever equation was relevant to explain Turing-Prigogine instability [1], pattern formation [1,34], localized structures [33,35,36], front dynamics [37,38] and spatiotemporal complex dynamics [39]. More recently, it has been shown that when taking into account the delay feedback, the LLE admits rogue waves and extreme events [40,41]. In this issue, some of our authors show that the formation of rogue waves can occur in the absence of delay feedback (see the paper by Panajotov et al., in this special issue). Figure 2 shows the typical bifurcation diagram of the Lugiato-Lefever equation with positive detuning in the bistable regime. The solid and the dashed curve account for the stable and the unstable uniform state, respectively. In addition, it is characterized the parameter region where localized structures and spatiotemporal chaos are observed numerically [39].

## 3 Localized structures and spatiotemporal chaos

From the envelope equation (3), it is easy to characterize analytically the uniform equilibria. The uniform steady state response $A$ of equation (3) satisfies $\gamma^2 = [\mu^2 + (\nu - |A|^2)]|A|^2$. for $\nu < \sqrt{3}\mu$, the steady, uniform state is a single valued function. For $\nu > \sqrt{3}\mu$ the system exhibits a bistable behavior with an S-shaped curve (see Fig. 2a). In contrast, in the driven damped sine-Gordon equation, the analytical characterization of uniform oscillations far from the quasi-reversible limit is a complex endeavor. Numerically, we have calculated the amplitude of a uniform oscillation as function of forcing $\gamma$ and have compared this oscillation amplitude with the oscillation

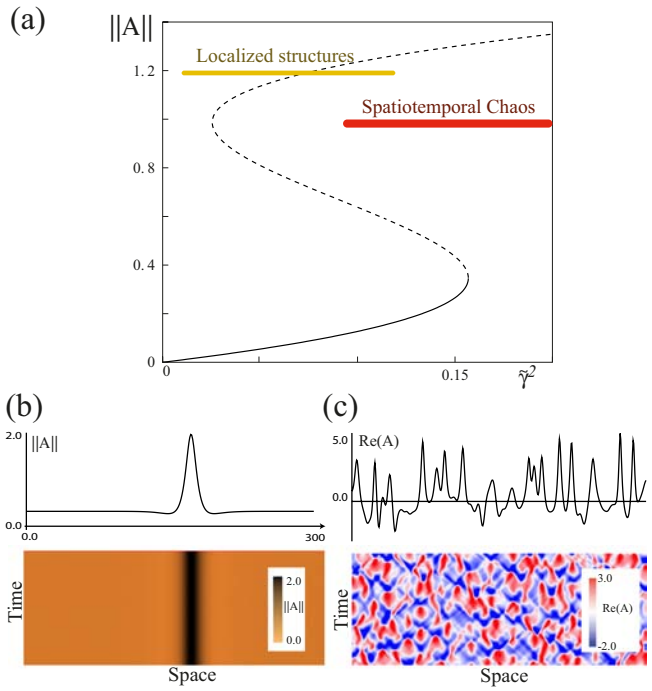


**Fig. 2.** The Lugiato-Lefever dynamics, equation (3). (a) Representative bifurcation diagram of Lugiato-Lefever equation (3) versus the forcing intensity for positive detuning in the bistable regime. The solid and the dashed curve account for the stable and the unstable uniform state. The colored bars account, respectively, for the parameter region where localized structures and spatiotemporal chaos are observed. (b) Instantaneous profile and spatiotemporal evolution of the amplitude $||A||$ for a localized structures. (c) Instantaneous profile and spatiotemporal evolution of $Re(A)$ in the spatiotemporal chaotic regime.

amplitude that one obtains considering a single pendulum, avoiding spatial instabilities of the chain of pendula. Figure 3a summarizes the comparison between oscillation amplitude of a single pendulum (solid and dashed curve) and the numerical values of the amplitude of a uniform oscillation (triangular symbols). The uniform oscillation experience a modulation instability. This bifurcation leads to the formation of standing waves solutions (cf. Fig. 4).

The upper branch of this curve accounts for an uniform oscillation with large amplitude. Similar bifurcation diagram has been obtained theoretically and experimentally in a driven damped array of coupled pendula [42,43]. Notwithstanding, this uniform oscillation is unstable as result of the Turing-Prigogine instability. Figure 3b displays the spatiotemporal evolution and a schematic representation of a uniform oscillation of the driven damped sine-Gordon model. Hence, the system exhibits a coexistence between a stable uniform oscillation and an unstable standing wave (cf. painted area of Fig. 3a).

In the coexistence area, one expects to observe localized structures [44–51], which correspond to localized waves [52]. In the context of Lugiato-Lefever equation (3), localized structures have been examined in one and in two dimensional LLE [33,35,53]. Figure 3d shows

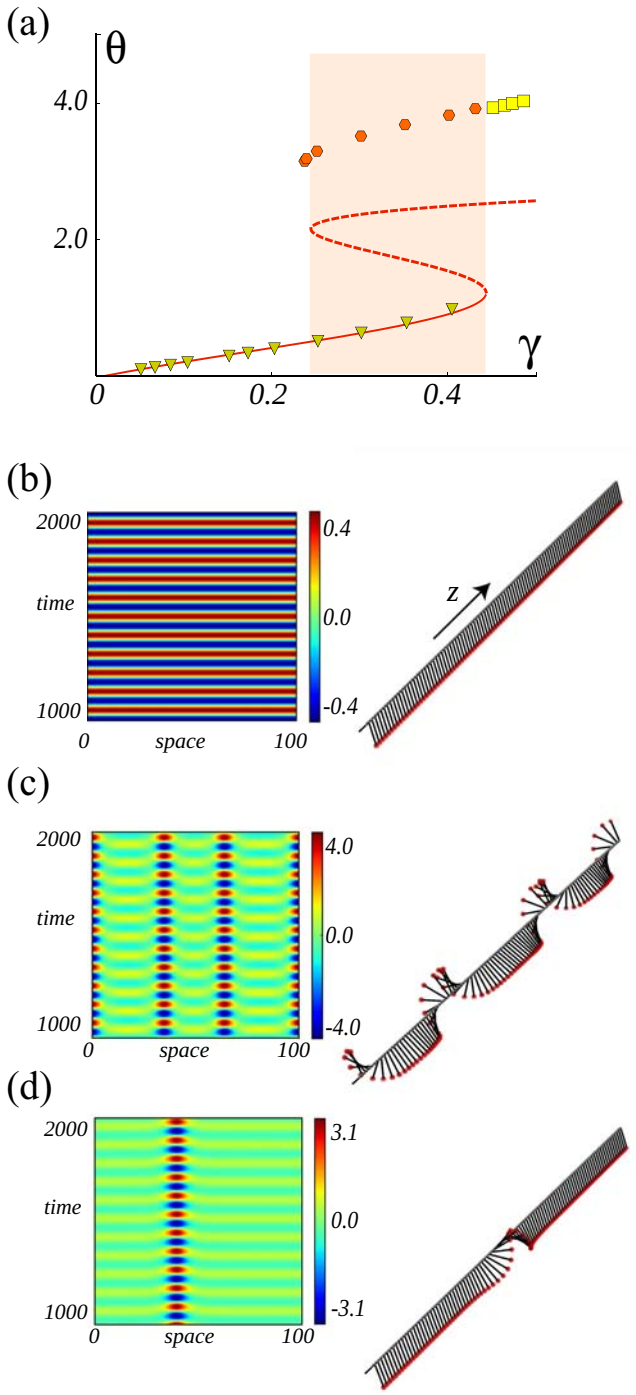


**Fig. 3.** Dynamics of the driven dissipative chain of pendula model equation (1). (a) Bifurcation diagram: the amplitude of the oscillation versus the forcing intensity $\gamma$. The solid and dashed curves account, respectively, for the stable and unstable uniform oscillation around the vertical state $\theta(x,t) = 0$. Triangular symbols corresponds to numerical observations of equation (1) with $\omega_0 = 1$, $\mu = 0.15$, $\kappa = 1$, $\omega = 2.7$, $dt = 0.05$ and $dx = 0.5$. Hexagonal and square symbols account for the maximum amplitude of localized structures and amplitude of the patterns, respectively. The painted area accounts for the coexistence region. Spatiotemporal evolution and schematic representation of an uniform oscillation $\gamma = 0.207$ (b), a standing wave $\gamma = 0.45$ (c), and a localized waves $\gamma = 0.3$ (d).

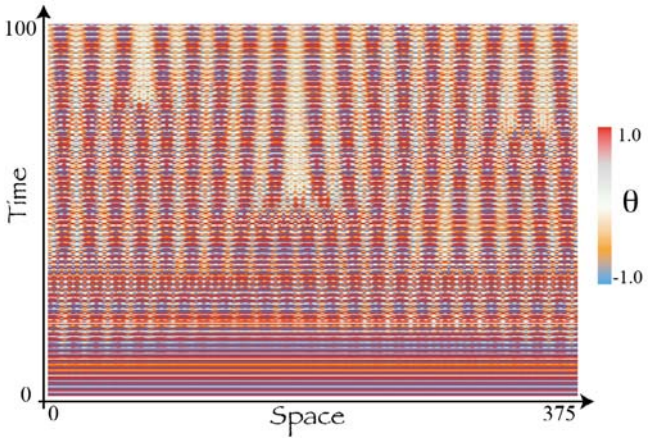


**Fig. 4.** Spatiotemporal evolution of modulational instability of a driven damped sine-Gordon equation (1) with $\omega_0 = 1.0$, $\mu = 0.09$, $\kappa = 1.0$, $\gamma = 0.8$, $\omega = 2.7$,$dt = 0.076$ and $dx = 0.75$.

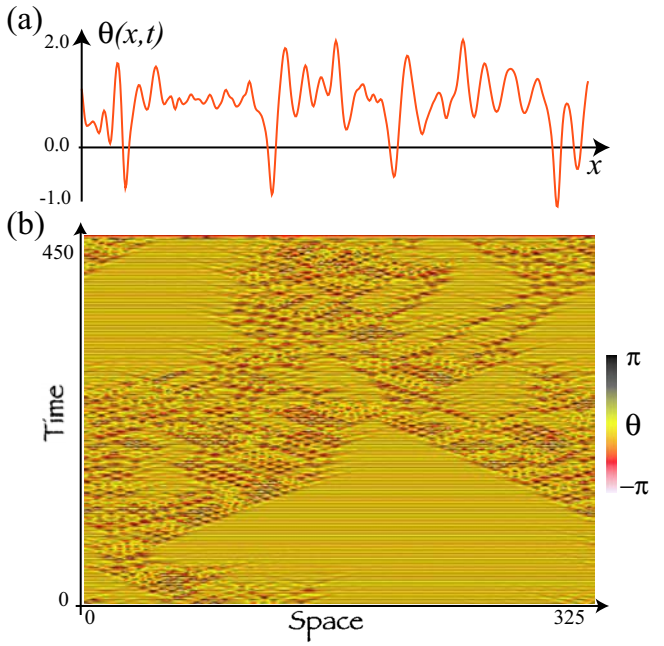


**Fig. 5.** Spatiotemporal intermittency of a driven dissipative chain of pendula equation (1) with $\omega_0 = 1.0$, $\mu = 0.0518$, $\kappa = 1.0$, $\gamma = 5.8$, $\omega = 2.7$, $dt = 0.057$ and $dx = 0.65$. (a) Instantaneous profile and (b) spatiotemporal diagram of $\theta(x,t)$.

the spatiotemporal evolution and a schematic representation of a localized waves in a driven dissipative chain of pendula. Experimentally, this type of structure has been observed in a forced damped array of coupled pendula [42,54]. From the uniform oscillation it is easy to obtain this localized state by considering a local perturbation. This particle type solutions are the dissipative counterpart of soliton solutions of the sine-Gordon equation [19,23]. The localized wave is characterized by a central peak accompanied laterally by two depressions in the amplitude (cf. Fig. 2b). The maximum of the amplitude of localized wave as function of the forcing intensity $\gamma$ is represented by hexagonal symbols in Figure 3a. For small strength of the forcing $\gamma$, these solutions appear by a saddle-node bifurcation. When increasing the forcing intensity these solutions becomes unstable by a radiation of complex spatiotemporal state [39,55]. Indeed, the localized waves obtained with the driven damped sine-Gordon equation and the Lugiato-Lefever model are quite similar.

Outside the coexistence region and large strength of the forcing $\gamma$, one can observe stable standing waves, which correspond to the counterpart of the pattern state observed in the Lugiato-Lefever equation. Figure 3c depicts the spatiotemporal evolution and a schematic representation of a standing wave. These solutions come out from the unstable uniform oscillation – upper branch in Figure 3a – as result of the modulational instability. Namely, from an initial homogeneous oscillation appears a small spatial modulation that increases systematically to a finite amplitude. However, this standing wave is unstable. It broke its spatial periodicity by several localized phase singularities, which allows the system to reach the adequate wavelength of the stable standing wave. Figure 4 illustrates the modulation instability process of a uniform oscillation. The phase singularities are recognizable by means of the dislocations observed in the spatiotemporal diagram [56]. In Figure 3a the square symbols stand for the amplitude of the stable standing waves.

Recently, it has been shown that for sufficiently large forcing the Lugiato-Lefever equation exhibits complex dynamical behaviors of spatiotemporal chaotic nature [39]. Likewise, it is well-known that a forced single pendulum with sufficient high forcing intensity exhibits chaotic behaviors of intermittent type [22]. Therefore, one expects that the driven dissipative sine-Gordon model, equation (1) also exhibits complex spatiotemporal behaviors. Chaotic behaviors of the driven damped sine-Gordon model have been extensively studied in the literature [57–63]. However, most of these studies are performed at the conservative limit. Likewise, tools used to characterize chaos as modal expansions, Poincaré section, time series of global quantities, leading Lyapunov exponents, temporal power spectra, correlation dimension, and dynamic structure factor are inadequate to study complex behaviors such as spatiotemporal chaos. An appropriate tool to characterize this type of behavior is the Lyapunov spectrum [64], which we will discuss later. Figure 5 shows the spatiotemporal evolution of the driven dissipative sine-Gordon model equation (1) for a large amplitude of forcing. Thus, one can infer that the chaotic behavior developed by this system is of a spatiotemporal intermittence type [65]. Because the system exhibits alternation of regular oscillations and irregular one. Moreover, the spatiotemporal diagram presents a Sierpinski-type structure. It is important to note that the spatiotemporal intermittency has not been reported in the context of the dynamics of the Lugiato-Lefever equation. Therefore, this dynamics is beyond the region of validity of this amplitude equation. For smaller values of the forcing intensity, we observe a complex spatiotemporal behavior more similar to that observed in the Lugiato-Lefever equation.

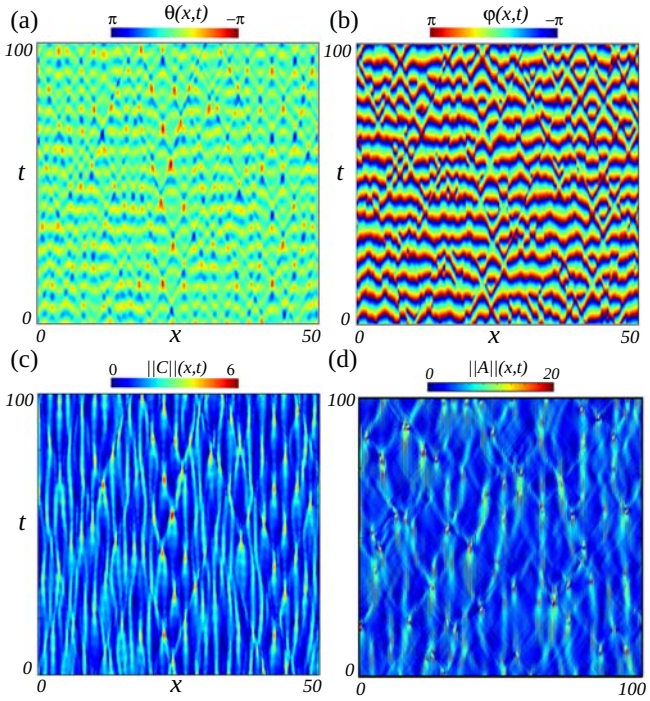


**Fig. 6.** Spatiotemporal chaos of a driven dissipative chain of pendula equation (1) with $\omega_0 = 1.0$, $\mu = 0.05$, $\kappa = 1.0$, $\gamma = 0.27$, $\omega = 2.9$, $dt = 0.01$ and $dx = 0.35$: (a) $\theta(x,t)$, (b) $\varphi[\theta]$ phase and (c) amplitude of the angle $\theta$ using Hilbert transform, respectively. (d) a Lugiato-Lefever equation (3) with $\tilde{\mu} = 0.16$, $\nu = 1.0$, and $\tilde{\gamma} = 0.1225$.

Figure 6 depicts the dynamics observed in this regime. In addition, Figure 6a show the spatiotemporal evolution of the angle $\theta(x,t)$. In order to characterize this complex spatiotemporal dynamics, we have computed the Hilbert transform [66]. From this transformation one can extract the amplitude, $||C||$=amplitude$[\theta(x,t)]$, and the phase $\varphi(x,t)$ of the oscillatory field $\theta(x,t)$. Figures 6b and 6c depict the respective phase and amplitude of the oscillatory field. The amplitude $||C||$ is characterized by present complex filament structure, which is the typical signature of the spatiotemporal chaotic regime. Figure 6d show the spatiotemporal evolution of the field amplitude of the Lugiato-Lefever equation. Therefore both systems exhibit similar qualitative dynamical behaviors, even though the amplitude equation (3) is far from the parameter region where it is valid as an approximation of the driven dissipative chain of pendula.

The characterization of complex dynamical behavior can be achieved by means of Lyapunov exponents, which provide an information about permanent dynamic with sensitivity of close initial conditions [64]. When the largest Lyapunov exponent is positive, the system develops a chaos but not necessarily a spatiotemporal chaos. To distinguish between these dynamical behaviors, it is necessary to determine the Lyapunov spectrum constitutes by the set of exponents. Spatiotemporal chaos has a Lyapunov spectrum with a continuous set of positive values. In contrast, chaos possesses a Lyapunov spectrum

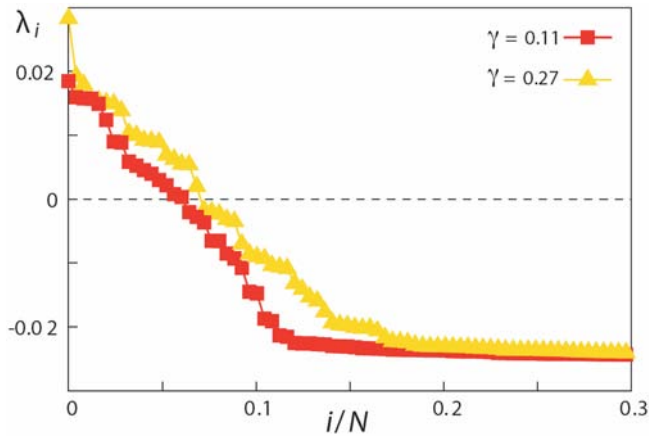


**Fig. 7.** Lyapunov spectra of a driven dissipative chain of pendula, equation (1), with $\omega_0 = 1.0$, $\kappa = 1.0$, $\mu = 0.05$ and $\omega = 2.9$ and different intensities forcing $\gamma$. $\lambda_i$ account for the different Lyapunov exponents, $i$ indexes the different exponents, and $N$ is the total number of considered pendula.

with a discrete set of positive values. The analytical computation of Lyapunov exponents is a complex endeavor and in practice inaccessible, then the logical strategy is a numerical derivation of the exponents. To study numerically the Lyapunov exponents is necessary to discretize equation (1) [67]. Let $N$ be the number of discretization points. We have computed numerically the Lyapunov spectrum of the driven damped sine-Gordon equation (1). Figure 7 shows the typical Lyapunov spectra of equation (1). $\lambda_i$ account for the different Lyapunov exponents, $i = \{0, 1, \ldots, N\}$ indexes the exponents with $\lambda_p \geq \lambda_q$ $(p > q)$, and $N$ is the total number of considered pendula. Therefore, we conclude that complex dynamical present by the driven dissipative chain of pendula is of spatiotemporal chaotic nature. It is worthy to note that a similar Lyapunov spectra is presented by Lugiato-Lefever equation [39].

## 4 Conclusions and comments

We have considered a mechanical system, namely a driven dissipative chain of pendula far from the conservative limit, and an extended Josephson junction. Both devices are described by the forced dissipative sine-Gordon model. From this equation, we have summarized the derivation of the Lugiato-Lefever equation. The LLE has been obtained in the time reversal limit perturbed with small injections and small dissipations of energy. We have qualitatively compared the dynamics obtained from the Lugiato-Lefever model with a forced dissipative sine-Gordon model. We have observed qualitatively similar bifurcation diagram for homogeneous, localized and pattern states. Unexpectedly, even the spatiotemporal chaotic dynamics are similar from both systems. Based on Lyapunov spectrum, we have established the spatiotemporal chaotic nature of the complex dynamics exhibited by a driven

dissipative chain of pendula and by an extended Josephson junction.

Time-periodically driven dynamical systems are a context where the qualitative understanding of the dynamics is still precarious. Few analytical results are accessible in general. The amplitude equations have been a systematic strategy to study this type of systems. Nonetheless, this type of analysis is only valid in narrow regions of the parameter space. Moreover, the predicted dynamics can qualitatively be observed far from the region of validity of envelope model equation such as the Lugiato-Lefever equation. This allows developing an intuition of the complex dynamics observed by time-periodically driven dynamical systems. Likewise, due to the advances of the amplitude equation in the context of optics, particularly the Lugiato-Lefever equation, it is possible to transfer knowledge from one research area to another toward a cross-fertilization between mechanical systems, extended Josephson junction, and both temporal and spatial nonlinear optical resonator.

M.G.C. and M.A.F. thank for the financial support of CONICYT-USA, project PII20150011. S.C. thanks the Interuniversity Attraction Poles program of the Belgian Science Policy Office under the grant IAPP7-35, the French Project ANR Blanc OptiRoc N12-BS04-0011, the "Laboratoire d'Excellence: Centre Européen pour les Mathéma-tiques, la Physique et leurs Interactions" CEMPI. MT received support from the Fonds National de la Recherche Scientifique (Belgium), and RGR, and SC thank financial support of ECOS-CONICYT project C15E06.

## Author contribution statement

All the authors worked on the theoretical description and discussed the results. M.A.F. performed the numerical simulations and analysis with inputs from M.G.C., R.R., and M.T.; S. C. developed the codes to determine the Lyapunov spectra and calculated them numerically. M.G.C. and M.A.F. developed and edited the figures. M.G.C. proposed to address this issue, and wrote the first draft with M.A.F.; all authors are actively involved in the writing of the final version of the article.

## References

1. L.A. Lugiato, R. Lefever, Phys. Rev. Lett. **58**, 2209 (1987)
2. D.W. McLaughlin, J.V. Moloney, A.C. Newell, Phys. Rev. Lett. **51**, 75 (1983)
3. D.W. McLaughlin, J.V. Moloney, A.C. Newell, Phys. Rev. Lett. **54**, 681 (1985)
4. A.M. Turing, Phil. Trans. R. Soc. Lond. B: Biol. Sci. **237**, 37 (1952)
5. I. Prigogine, R. Lefever, J. Chem. Phys. **48**, 1695 (1968)
6. P. Glansdorff, I. Prigogine, *Thermodynamic Theory of Structure, Stability and Fluctuations* (NY Interscience, New York, 1971)
7. P. Kockaert, P. Tassin, G. Van der Sande, I. Veretennicoff, M. Tlidi, Phys. Rev. A **74**, 033822 (2006)
8. U. Peschel, O. Egorov, F. Lederer, Opt. Lett. **29**, 1909 (2004)
9. M. Haelterman, S. Trillo, S. Wabnitz, Opt. Commun. **91**, 401 (1992)
10. Y.K. Chembo, C.R. Menyuk, Phys. Rev. A **87**, 053852 (2013)
11. T. Hansson, D. Modotto, S. Wabnitz, Phys. Rev. A **88**, 023819 (2013)
12. A. Coillet, J. Dudley, G. Genty, L. Larger, Y.K. Chembo, Phys. Rev. A **89**, 013835 (2014)
13. M. Tlidi, M. Haelterman, P. Mandel, Europhys. Lett. **42**, 505 (1998)
14. M. Tlidi, M. Haelterman, P. Mandel, Quant. Semiclass. Opt.: J. Eur. Opt. Soc. B **10**, 869 (1998)
15. P. Tassin, G. Van der Sande, N. Veretenov, P. Kockaert, I. Veretennicoff, M. Tlidi, Opt. Express **14**, 9338 (2006)
16. G.J. Morales, Y.C. Lee, Phys. Rev. Lett. **33**, 1016 (1974)
17. K. Nozaki, N. Bekki, Phys. Lett. A **102**, 383 (1984)
18. D.J. Kaup, A.C. Newell, Phys. Rev. B **18**, 5162 (1978)
19. G. Terrones, D.W. McLaughlin, E.A. Overman, A.J. Pearlstein, SIAM J. Appl. Math. **50**, 791 (1990)
20. L.D. Landau, E.M. Lifshitz, *Mechanics, Course of Theoretical Physics* (Pergamon Press, 1976), Vol. 1
21. A. Frova, M. Marenzana, *Thus spoke Galileo: the great scientist's ideas and their relevance to the present day* (Oxford University Press, 2006)
22. G.L. Baker, J.A. Blackburn, *The pendulum: a case study in physics* (Oxford University Press, 2005)
23. Y.S. Kivshar, B.A. Malomed, Rev. Mod. Phys. **61**, 763 (1989)
24. N.N. Bogoliubov, Y.A. Mitropolski, *Asymptotic methods in the theory of non-linear oscillations* (Gordon and Breach, New York, 1961)
25. J. Cuevas-Maraver, P.G. Kevrekidis, F. Williams, *The Sine-Gordon Model and its Applications* (Springer, 2014)
26. D. Bennett, A. Bishop, S. Trullinger, Zeitschrift für Physik B Condensed Matter **47**, 265 (1982)
27. L.P. Gor'kov, G. Grüner, *Charge density waves in solids* (Elsevier, 2012), Vol. 25
28. O.M. Braun, Y. Kivshar, *The Frenkel-Kontorova model: concepts, methods, and applications* (Springer Science & Business Media, 2013)
29. E. Berrios-Caro, M.G. Clerc, A.O. Leon, Phys. Rev. E **94**, 052217 (2016)
30. M. Clerc, P. Coullet, E. Tirapegui, Phys. Rev. Lett. **83**, 3820 (1999)
31. M. Clerc, P. Coullet, E. Tirapegui, Opt. Commun. **167**, 159 (1999)
32. M. Clerc, P. Coullet, E. Tirapegui, Int. J. Bifurc. Chaos **11**, 591 (2001)
33. I.V. Barashenkov, Y.S. Smirnov, Phys. Rev. E **54**, 5707 (1996)
34. M. Tlidi, R. Lefever, P. Mandel, Quant. Semiclass. Opt.: J. Eur. Opt. Soc. B **8**, 931 (1996)
35. A.J. Scroggie, W.J. Firth, G.S. McDonald, M. Tlidi, R. Lefever, L.A. Lugiato, Chaos Solitons Fract. **4**, 1323 (1994)
36. I.V. Barashenkov, Y.S. Smirnov, N.V. Alexeeva, Phys. Rev. E **57**, 2350 (1998)
37. S. Coen, M. Tlidi, P. Emplit, M. Haelterman, Phys. Rev. Lett. **83**, 2328 (1999)
38. S. Coulibaly, M. Taki, M. Tlidi, Opt. Express **22**, 483 (2014)

39. Z. Liu, M. Ouali, S. Coulibaly, M. Clerc, M. Taki, M. Tlidi, Opt. Lett. **42**, 1063 (2017)
40. N. Akhmediev, B. Kibler, F. Baronio, M. Beli, W.P. Zhong, Y. Zhang, W. Chang, J.M. Soto-Crespo, P. Vouzas, P. Grelu et al., J. Opt. **18**, 063001 (2016)
41. M. Tlidi, K. Panajotov, Chaos: Interdiscip. J. Nonlinear Sci. **27**, 013119 (2017)
42. F. Palmero, J. Han, L.Q. English, T. Alexander, P. Kevrekidis, Phys. Lett. A **380**, 402 (2016)
43. Y. Xu, T.J. Alexander, H. Sidhu, P.G. Kevrekidis, Phys. Rev. E **90**, 042921 (2014)
44. M. Tlidi, M. Taki, T. Kolokolnikov, Chaos: Interdiscip. J. Nonlinear Sci. **17**, 037101 (2007)
45. O. Descalzi, M.G. Clerc, S. Residori, G. Assanto, *Localized states in physics: solitons and patterns* (Springer-Verlag Berlin Heidelberg, 2011)
46. H.G. Purwins, H. Bdeker, S. Amiranashvili, Adv. Phys. **59**, 485 (2010)
47. M. Tlidi, K. Staliunas, K. Panajotov, A.G. Vladimirov, M.G. Clerc, Phil. Trans. R. Soc. Lond. A: Math. Phys. Eng. Sci. (2014)
48. L. Lugiato, P. Franco, M. Brambilla, *Nonlinear Optical Systems* (Cambridge University Press, 2015)
49. D. Mihalache, Rom. Rep. Phys. **67**, 1383 (2015)
50. Y. He, X. Zhu, D. Mihalache, Rom. J. Phys. **61**, 595 (2016)
51. D. Mihalache, Rom. Rep. Phys. **69**, 403 (2017)
52. M.G. Clerc, S. Coulibaly, D. Laroze, EPL **97**, 30006 (2012)
53. I. Barashenkov, E. Zemlyanaya, Phys. D: Nonlinear Phenom. **132**, 363 (1999)
54. J. Cuevas, L.Q. English, P.G. Kevrekidis, M. Anderson, Phys. Rev. Lett. **102**, 224101 (2009)
55. F. Leo, L. Gelens, P. Emplit, M. Haelterman, S. Coen, Opt. Express **21**, 9180 (2013)
56. M.G. Clerc, C. Falcón, M.A. García-Ñustes, V. Odent, I. Ortega, Chaos: Interdiscip. J. Nonlinear Sci. **24**, 023133 (2014)
57. A.R. Bishop, K. Fesser, P.S. Lomdahl, W.C. Kerr, M.B. Williams, S.E. Trullinger, Phys. Rev. Lett. **50**, 1095 (1983)
58. A.R. Bishop, M.G. Forest, D.W. McLaughlin, E. Overman, Phys. D: Nonlinear Phenom. **23**, 293 (1986)
59. E. Overman, D.W. McLaughlin, A.R. Bishop, Phys. D: Nonlinear Phenom. **19**, 1 (1986)
60. A.R. Bishop, D. McLaughlin, M.G. Forest, E.A. Overman, Phys. Lett. A **127**, 335 (1988)
61. A. Bishop, M.G. Forest, D. McLaughlin, E. Overman, Phys. Lett. A **144**, 17 (1990)
62. A.R. Bishop, R. Flesch, M.G. Forest, D.W. McLaughlin, E.A. Overman, II, SIAM J. Math. Anal. **21**, 1511 (1990)
63. A. Gavrielides, T. Kottos, V. Kovanis, G.P. Tsironis, Phys. Rev. E **58**, 5529 (1998)
64. A. Pikovsky, A. Politi, *Lyapunov Exponents: A Tool to Explore Complex Dynamics* (Cambridge University Press, 2016)
65. H. Chaté, Nonlinearity **7**, 185 (1994)
66. J.F. Claerbout, *Fundamentals of Geophysical Data Processing* (McGraw-Hill, New York, 1976)
67. M.G. Clerc, N. Verschueren, Phys. Rev. E **88**, 052916 (2013)